AD_____

Award Number: W81XWH-09-1-0276

TITLE: Therapeutic Remyelination Strategies in a Novel Model of Multiple Sclerosis: Japanese Macaque Encephalomyelitis

PRINCIPAL INVESTIGATOR: Larry S. Sherman, Ph.D.

CONTRACTING ORGANIZATION: Oregon Health & Science University
Beaverton, OR 97006

REPORT DATE: Annual

TYPE OF REPORT: May 2012

PREPARED FOR: U.S. Army Medical Research and Materiel Command
Fort Detrick, Maryland 21702-5012

REPORT DOCUMENTATION PAGE

Form Approved
OMB No. 0704-0188

1. REPORT DATE	2. REPORT TYPE	3. DATES COVERED
May 2012	Annual	1 May 2011 – 30 April 2012

4. TITLE AND SUBTITLE

Therapeutic Remyelination Strategies in a Novel Model of Multiple Sclerosis: Japanese Macaque Encephalomyelitis

5a. CONTRACT NUMBER

5b. GRANT NUMBER
W81XWH-09-1-0276

5c. PROGRAM ELEMENT NUMBER

6. AUTHOR(S)

Larry S. Sherman, Scott Wong, Betsy Ferguson, William Rooney

E-Mail: shermanl@ohsu.edu

5d. PROJECT NUMBER

5e. TASK NUMBER

5f. WORK UNIT NUMBER

7. PERFORMING ORGANIZATION NAME(S) AND ADDRESS(ES)

Oregon Health & Science University
Beaverton, OR 97006

8. PERFORMING ORGANIZATION REPORT NUMBER

9. SPONSORING / MONITORING AGENCY NAME(S) AND ADDRESS(ES)
U.S. Army Medical Research and Materiel Command
Fort Detrick, Maryland 21702-5012

10. SPONSOR/MONITOR'S ACRONYM(S)

11. SPONSOR/MONITOR'S REPORT NUMBER(S)

12. DISTRIBUTION / AVAILABILITY STATEMENT
Approved for Public Release; Distribution Unlimited

13. SUPPLEMENTARY NOTES

14. ABSTRACT

During the second year of this grant, we have finished characterizing the spontaneous form of Japanese macaque encephalomyelitis (JME) and published a manuscript in Annals of Neurology describing our results; we have characterized how intracranial injections of the Japanese macaque rhadinovirus (JMRV) induce demyelinating disease, as assessed by histopathology, MRI, and symptoms; we have demonstrated both in vitro and in vivo which cells are affected by JMRV infection; we have performed additional analyses characterizing the immune response to JMRV infection; and we have continued our genetic analyses. In the next year, we will continue to analyze the mechanisms by which JMRV triggers disease onset and immune responses and the role of the cytopathic effects of the virus in this process, which genes are linked to disease susceptibility, and how the virus influences cells in lesion microenvironments.

15. SUBJECT TERMS
multiple sclerosis, Japanese macaque, demyelination, virus, major histocompatibility complex

16. SECURITY CLASSIFICATION OF:			17. LIMITATION OF ABSTRACT	18. NUMBER OF PAGES	19a. NAME OF RESPONSIBLE PERSON
a. REPORT	b. ABSTRACT	c. THIS PAGE			USAMRMC
U	U	U	UU	27	19b. TELEPHONE NUMBER *(include area code)*

Table of Contents

INTRODUCTION

Multiple Sclerosis (MS) is characterized by autoimmune destruction of myelin sheaths and axons, leading to conduction deficits that influence motor, sensory and cognitive function. Although the etiology of MS is still poorly understood, particular viruses, especially gama-herpes viruses, may act as a trigger for MS (Levin et al., 2010; Ascherio and Munger, 2010). Furthermore, there is growing evidence that susceptibility to MS may be linked to polymorphisms at certain genetic loci, including major histocompatibility complex (MHC) genes and the interleukin-7a gene (Ramagopalan et al., 2009; Harley, 2007).

This study is a collaborative effort between several investigators at the Oregon National Primate Research Center (ONPRC) who are interested in understanding the pathophysiological mechanisms that trigger MS and related inflammatory demyelinating disease. We have characterized a novel encephalomyelitis that occurs spontaneously in a small percentage of animals in a colony of Japanese macaques (JMs) at the ONPRC (Axthelm et al., 2011). The disease, called Japanese macaque encephalomyelitis (JME), occurs in both progressive and relapsing-remitting forms and is characterized by brain and spinal cord demyelination and axonopathy that is accompanied by extensive astrogliosis. Affected animals develop debilitating motor and ocular disturbances. Approximately 10% of the animals in this colony appear to have chronic, subclinical lesions as evaluated by magnetic resonance imaging (MRI). Pedigree analysis indicates that particular lineages of animals are substantially more susceptible to this disease than others, suggesting a genetic pre-disposition to JME. Furthermore, we have cloned a gamma-herpes virus (called Japanese macaque rhadovirus; JMRV) from animals in this colony that is found within demyelinated JME lesions.

This highly integrated, multidisciplinary application is focused on developing JME as a pathophysiogical and genetic model of MS whose etiology and progression more closely resemble MS in humans than other EAE and viral models in non-human primates and rodents. We aim to use this model to better understand how gamma-herpes viruses trigger demyelination and axon damage; whether polymorphisms in gene loci that have been linked to MS in humans also predispose JMs to JME; to evaluate the lesions in both symptomatic and subclinical animals to determine if they model numerous aspects of human MS lesions; and to test if gamma-herpes virus infection directly influences astrogliosis and the accumulation of factors, such as hyaluronan, that can inhibit remyelination in demyelinated lesions. Our long-term goal is to develop JME as a model for testing immunological and neurobiological processes underlying MS, and to use this model in pre-clinical screens of novel agents with the potential to inhibit MS attacks and to promote remyelination and regeneration.

We have requested a no-cost extension to complete these studies with the aim of having sufficient data to publish all of our findings within the next year.

BODY

Task 1: To test the hypothesis that intracranial infection with JMRV can experimentally induce JME.

a. *Test effects of intracranial JMRV infection of 20 JMs from previously affected lineages; perform clinical, MRI, and immunologic assessments*
b. *Test effects of JMRV infections in additional (up to 24) JMs selected based on genetic analyses in aim 2 or from additional pedigree analyses.*

We have experimentally inoculated a total of 29 animals through year 3 of the award. Each of the Japanese macaques (JMs) received a series of MRIs pre- and post-infection to document and assess the inflammatory response to intracranial inoculation (i.c.). The animals were separated into two groups based upon whether they were genetic or observed 1st order relatives (related, n=17) of animals that developed spontaneous JME or non-related animals (not related, n=12). The extent of the inflammatory response in the white matter (WM) as determined by hyperintensive T_2–weighed signal, was calculated volumetrically as percent WM affected and is presented as line graphs of related and not related (Fig 1A).

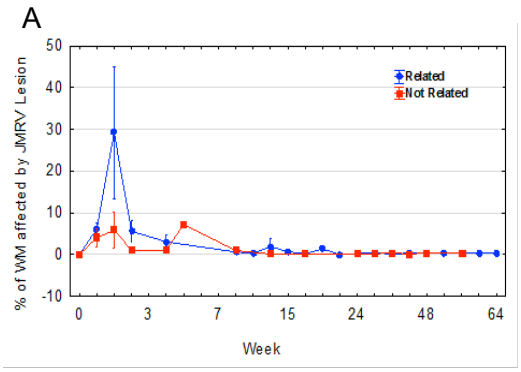

Fig 1. Comparison of affected WM following intracranial JMRV infection (A) or vehicle alone (B) in 1st order relatives of spontaneous JME affected animals versus non-related animals. Percent of WM affected from each animal in the related or not related was determined by T2-weighted signal acquired by MRI analysis. The mean for each group was calculated at each time post-infection (week) along with the standard deviation.

By this analysis we found that related JMs achieved a statistically significant ($p \leq 0.0001$) increase in T_2-weighted signal in the WM compared to JMs that were not related at 1 week post-infection. These findings suggest the related JMs are more susceptible to inflammatory responses following i.c. virus infection as there was no difference in T_2-weighed signal by vehicle injection alone in either group (Fig 1B). These results were substantiated by statistical analysis.

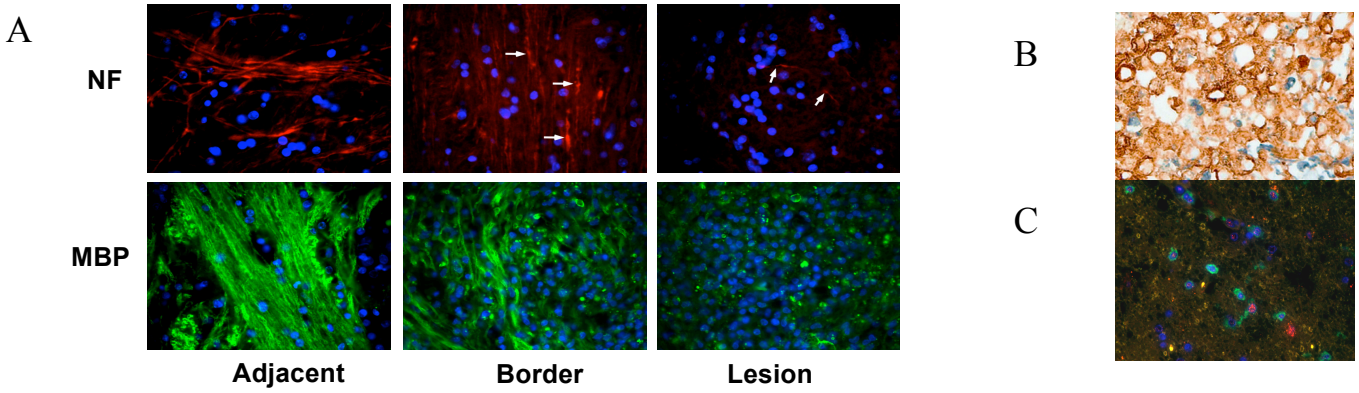

Fig 2. **A**. High magnification images of the lesion, border and unaffected white matter stained for the presence of MBP, NF and DAPI for nuclei to visualize the extent of demyelination and axonal damage. Note reduction in MBP and NF staining in both the lesion and border areas. The merged image of lesion and border reveals increased cellularity (increased DAPI staining), some preserved myelinated axons and some NF+ axons without myelin. **B**. IHC of lesion site with antibodies specific for CD163 (macrophage, brown) and MBP (grayish blue). **C**. IFA of lesion showing JMRV MCP staining (red) in IBA-1+ microglia and activated macrophages (green). All images are at 400x magnification.

Interestingly, despite the presence of significant inflammation in the hemisphere inoculated with virus in the related JMs, only two of the related JMs displayed clinical symptoms associated with the infection. One animal developed paralysis on day 8 and was euthanized and the other displayed some neurologic deficits, but these deficits resolved within a few days and the animal recovered. **Fig 2** demonstrates the inflammation associated with i.c. JMRV infection in the brain isolated from the animal that was humanely euthanized, accompanied by extensive demyelination and axonopathy. Similar to human lesions, JMRV-induced lesions also demonstrated elevated hyaluronan, which has been implicated in remyelination failure (Back et al., 2005).

Since the related JMs reacted differently than the not related animals, we investigated whether the animals differed in their T cell-mediated immune response to JMRV infection. To accomplish this, we performed intracellular cytokine staining (ICS) assays on peripheral mononuclear cells (PBMCs) isolated at different times post-infection that were consistent with MRI analysis. For this assay, isolated PBMCs are infected with JMRV in vitro and subsequently stained for interferon gamma (IFNγ) and for specific T cell subsets (CD4 or CD8+ T cells). By this analysis we found striking differences in CD4 (Fig 3A) and CD8 (Fig 3B) T cell responses to JMRV infection between related and not related animals. Specifically, JMRV-specific CD4+ and CD8+ T cell responses were detected earlier (3 weeks) in related animals than not related animals.

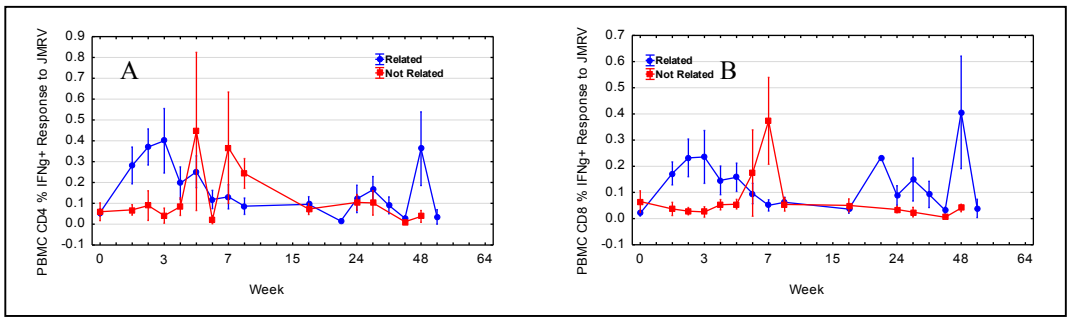

Fig 3: Comparison of CD4+ (**A**) and CD8+ (**B**) T cell responses to JMRV infection in related versus non-related animals. Percent of CD4 or CD8 T cells responding to JMRV infection was determined by ICCS and flow cytometry. The mean for each group was calculated at each time post-infection (week) and plotted along with the standard deviation.

Overall, these results support our hypothesis that experimental i.c. inoculation of JMs derived from specific lineages associated with development of JME with JMRV can precipitate inflammatory response which we believe can lead to inflammatory demyelination. We are currently evaluating whether these JMs develop immune responses to myelin components; specifically, myelin oligodendrocyte glycoprotein (MOG), myelin basic protein (MBP) and proteolipid protein (PLP).

Advanced MR Imaging of Japanese Macaque Encephalomyelitis

Non-invasive characterization of tissue represents an important approach to track pathophysiological changes in individual animals. In this project, we have developed and refined several powerful MRI techniques to characterize tissue vascular properties, determine myelin content, and compute lesion volumetrics including interstitial volume. Together, these measures offer a unique window to investigate pathological processes associated with neuroinflammation. These techniques have allowed us to determine that JME lesions share many radiological and pathological features with human multiple sclerosis. Specifically, in the acute JME lesion we find increased blood-brain barrier permeability (by 1000x compared to normal value) to a gadolinium based contrast agent, lesion blood volume increased up to 3x compared to normal values, interstitial volumes (vasogenic edema) increased 3x compared to normal values, and myelin content reduced up to 5x - although interestingly, most of the JME lesion volume reports near-normal myelin content in the early days after acute onset. Taken together, these techniques provide novel insights into spatio-temporal aspects of JME lesion formation including clear signatures of greatly increased blood volume (possibly angiogenesis), edema and regional demyelination. We currently are applying these

techniques to the cohort of JM animals inoculated with JMRV intracranially. Below we describe the measurement techniques and provide examples from a JM individual with acute JME.
All JM MRI data were collected using a Siemens 3T MRI instrument located on the campus of the ONPRC. The following sequences were acquired: 1) a coronal T_1-weighted 2D gradient recalled echo sequence (TR: 23 ms, TE: 7.39 ms, FA: 30°, field-of-view (FOV) 192 mm x 192 mm, matrix: 128x128), 2) a sagittal proton-density (PD) turbo spin echo (TSE) sequence (TR: 10000 ms; TE: 17 ms; echo train length (ETL) 9; FOV 192 mm x 192 mm, matrix: 256x256, slice thickness (ST) 1.5 mm), 3) an axial 2D T_2-weighted TSE sequence (TR: 9000 ms; TE: 51 ms; ETL 9, FOV 180 mm x 160 mm, matrix: 320x240, ST 1.0 mm), 4) an axial 2D PD TSE sequence (TR: 9000 ms, TE: 13 ms, ETL 9, FOV 180 mm x 160 mm matrix: 320x240, ST 1.0 mm), 5) a 2D transverse FLAIR (FLuid Attenuated Inversion Recovery) sequence, 6) an axial single slice 2D gradient recalled echo with 24 echo times (2.1 ≤ TE ≤ 63 ms, TR: 100 ms, FA: 15° FOV: 140 mm x 160 mm matrix: 96 x 128), and 7) a 3D T_1-weighted magnetic prepared rapid acquisition gradient echo (MPRAGE) sequence (TR: 2500 ms; TI: 900 ms; TE: 3.49 ms; FA: 8°; FOV 130 mm x 97.5 mm x 96 mm, matrix: 192x144x96). For quantitative T_1 estimation of cerebral ^1H_2O and pharmacokinetic (PK) modeling of tissue uptake of a low-molecular weight gadolinium based contrast agent (gadoteridol, see below), the MPRAGE series is extended to include TI values of 200 ms, 900 ms, 2200 ms, and an acquisition with no inversion preparation. The T_1-weighted MPRAGE acquisition was repeated approximately ten minutes after the i.v. administration of 0.1 mmol/kg gadoteridol (ProHance; Bracco Diagnostics, Inc) for qualitative evaluation, or at 10, 20, and 30 minutes post-gadoteridol administration for quantitative PK analysis. Quantitative T_1 maps were calculated from the MPRAGE series by iteratively solving the Bloch equations with appropriate incorporation of all radiofrequency pulses and delay periods inherent in the acquisitions. For longitudinal MRI studies, all volumetric image sets collected were spatially co-registered to a reference MPRAGE data set collected during the initial visit. Coregistration was achieved using the FSL FLIRT tool (http://www.fmrib.ox.ac.uk/fsl/flirt/index.html) with the following settings: correlation ratio cost function, six degrees of freedom, sinc interpolation for the output images, and a limited grid search.

Figure 4 shows anatomical MR image appearance for an acute JME lesion. This lesion shows evidence of a hemorrhagic core which appears hypointense on the T_2-w, PD-w, and FLAIR images. **Figure 5** illustrates tissue property estimations from MRI base and parametric images. Tissue volumetrics including T_2-w, PD-w, FLAIR, T_1-w and gadolinium enhancing lesion volume can all readily be determined. Tissue water T_1 values can also be obtained and we find 0.88 s, 1.30 s, and 1.20 s for white matter, gray matter, and JME lesion areas; very similar to values obtained from human brain at 3T. In **Figure 6** we quantify JME lesion properties using a dynamic contrast enhanced (DCE) MRI approach. This technique allows us to determine tissue blood volume fraction (p_b), interstitial volume fraction (v_e), and gadoteridol extravasation rate constant (K^{trans}). Lastly, we apply a quantitative relaxometric approach to estimate myelin water fraction. In **Figure 7** we show data from a 3T MRI multi-gradient recalled echo sequence (see sequence 6 above) in JME to estimate the fractional value of myelin associated water. To accomplish this, we assign the ^1H_2O signal component with a large R_2* value (≥ 100 s^{-1}) to be myelin associated water; an approach described by several other investigator groups (Du, et al 2007, van Gelderen, et al, 2012, Labadie, et al 2011). In **Figure 7** we plot the TE series obtained from regions-of-interest (ROI) located in several tissue types identified on FLAIR image including normal appearing white matter, normal appearing gray matter, and different regions with an acute JME lesion. The average values of ^1H_2O signal with large R_2* were found to be 7.7(1.4) for NAWM; 1.3(0.3) for NAGM, 5.3(1.9) for rim of acute JME lesion, and 1.0(2.6) of core of acute JME lesion (values in mean % (standard deviation)). These normal appearing tissue values are in excellent agreement with myelin water fraction estimates in the literature (Du, et al 2007). However, since the total water content of the acute lesion rim is increased (likely representing vasogenic edema) to 0.85 g water/(g tissue) from 0.70 g water/(g NAWM) (~20% increase as determined from PD-w and T2-w MRI), the apparent decrease in nominal MWF (i.e. uncorrected for edema) overestimates true loss of myelin. For the tissue regions presented in **Figure 7** we estimate the absolute average myelin associated water as 0.051(0.009) g/(g NAWM), 0.046(0.016) g/(g rim lesion), and 0.008(0.020) g/(g lesion core). For this acute JME lesion, only the core shows a

significant decrease in myelin associated water compared to NAWM. Interestingly, the lesion core also shows evidence of hemorrhage and this was primarily manifest in the small R_2 component which was increased to 24.6(2.1) s^{-1} compared to 20.1(1.6)s^{-1} for NAWM, and 13.9(1.9) s^{-1} for lesion rim.

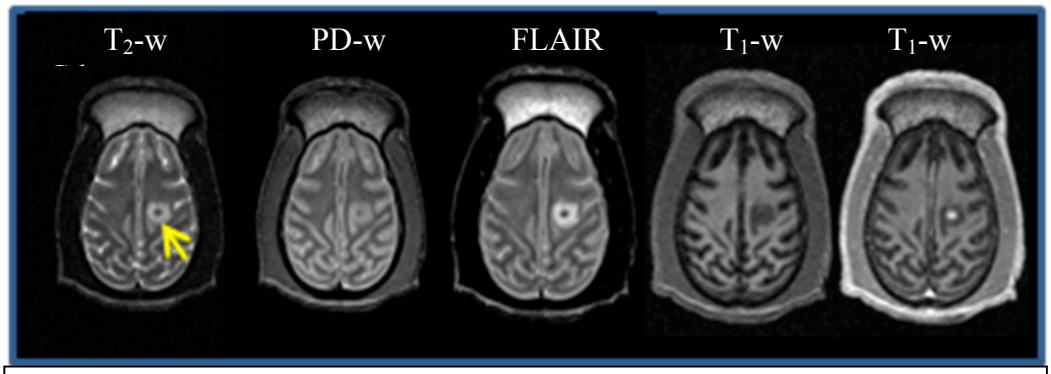

Figure 4. Transverse anatomical images from the same spatial location acquired from an animal with acute JME are displayed. The tissue contrast achieved by the different sequences (see above for full description) is clearly apparent. This lesion shows evidence of a hemorrhagic core which appears hypointense on the three left-most images. The right-most image shows this same region takes up substantial gadolinium contrast uptake indicative of a broken blood-brain barrier.

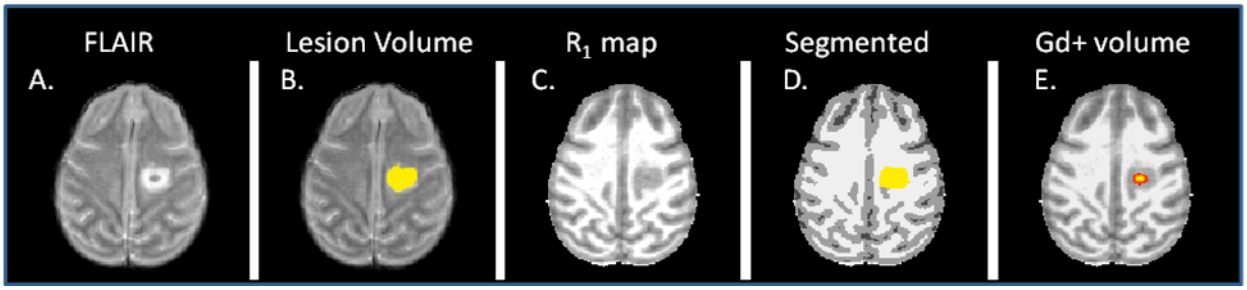

Figure 5. Example of tissue morphometric analysis in JME brain. The FLAIR image is used to identify WM signal hyperintensities which are classified as lesion volume. R_1 maps are generated by solving the Bloch equations as described in text. Tissue segmentation of the R1 maps into gray matter, white matter and cerebrospinal fluid was carried out using histogram inspection along with an automated segmentation tool [2]. These segmented images were manually edited to reclassify hypointense lesions within the white matter that had been misclassified as gray matter. Contrast enhanced images were created by subtracting pre-contrast R_1 maps from post-contrast R_1 maps and manually delineating regions of high delta R_1 within brain tissue, excluding major vessels. These regions of contrast enhancement were then overlaid on the pre-contrast R_1 map. For this individual we estimate the tissue properties: 54.6% normal appearing gray matter, 34.9% normal appearing white matter; 10% cerebrospinal fluid, and 0.6% lesion.

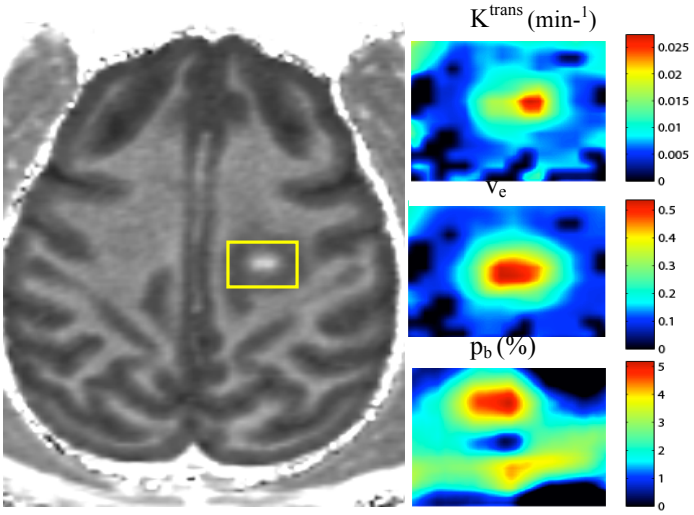

Figure 6. The left panel shows a T_1-w image acquired 40 minutes post gadoteridol injection in an acute JME case. The centrum semiovale white matter lesion outlined by yellow box shows marked signal enhancement consistent with a broken blood-brain barrier (BBB). The lesion properties were quantified using DCE-MRI. The top color image shows the lesion and surrounding tissue K^{trans} map with scale bar at right. The maximum K^{trans} observed for this lesion was ~0.03 min^{-1}, consistent with human multiple sclerosis. The middle color panel shows the gadoteridol distribution volume fraction map, mostly the interstitial volume or extravascular extracellular volume fraction (v_e) with values at the lesion core that approach 0.5. The bottom color image shows the blood volume fraction (p_b) map. The p_b map was calculated during the first pass of contrast agent and was corrected for leakage. Interestingly, the lesion blood volume maximum value approach 5% which is nearly 3x that of contralateral normal appearing white matter that had a mean value of 1.7% (data not shown). The marked increase in blood volume and leaky nature of blood vessels is consistent with angiogenesis.

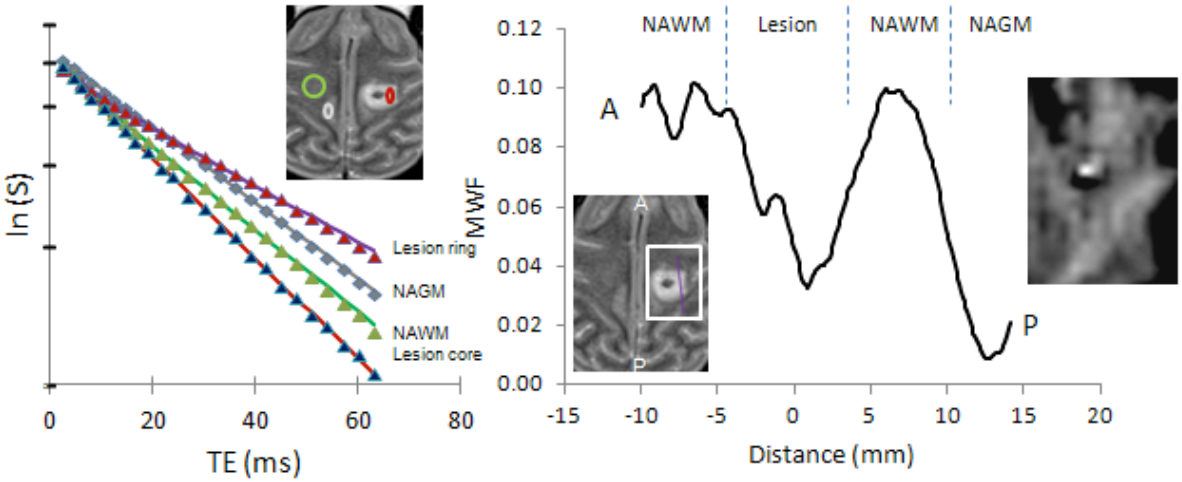

Figure. 7. Myelin water fraction (MWF) determination in and around an acute JME lesion. The left panel plot shows the signal intensity change (solid symbols) with echo time (TE) for 4 tissue ROIs (see inset) with solid lines that represent best fits of a biexponential decay function. The amplitude of the $R_2^* \geq 100$ s^{-1} component is assigned to MWF. The plot in the right panel shows how MWF fraction changes across an acute JME lesion. The plot traces the projection indicated by the solid line in the inset FLAIR image, from anterior (A) to posterior (P). In NAWM adjacent to hyperintense lesion on FLAIR MWF is approximately 0.10 and in the lesion is as low as ~0.03. The inset at the far right represent a MWF for the white rectangular ROI indicated in the FLAIR image.

Task 2: Test the hypothesis that common genetic variants in the JM genome increase the susceptibility of developing demyelinating disease.

Analysis of MHC haplotype association with disease susceptibility

Our initial investigation of associations between MHC haplotype and JME susceptibility utilized a set of 14 linked microsatellite/short tandem repeat (STR) markers that span the entire macaque MHC locus to broadly characterized MHC diversity. The survey of 288 Japanese macaques included 27 spontaneously occurring JME affected animals, 4 experimentally induced JME affected animals, and 7 animals without clinical symptoms, but with evidence for brain lesions by MRI analysis (MRI+). The study set also included 161 unaffected first-degree relatives (dams, sires, siblings or offspring) of JME affected animals, 48 unaffected first-degree relatives of MRI+ animals and 41 unaffected animals with no known first-degree JME relatives. The STR genotypes revealed 24 different haplogroups, each carrying the same STR alleles throughout the MHC region. Less than 10% of animals exhibited recombination between distal markers. Only 13 of the 24 MHC possible haplogroups were carried by JME affected animals.

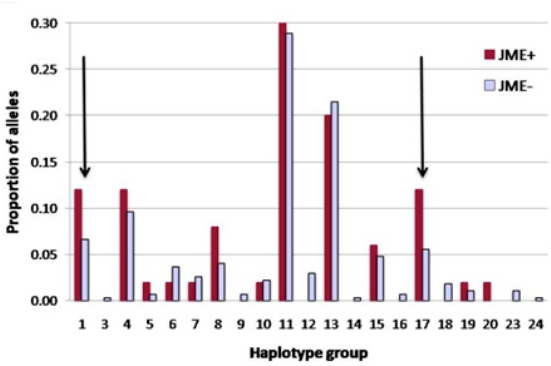

Figure 8. Distribution of MHC STR haplogroups among JME cases and non-affected controls.

Table 1. Expressed DRB alleles in 26 Japanese macaques.

STR Group	*Mafu-DRB*
11, 13	*DRB*001:nov:01* *DRB*003:nov:01*
15*, 17*	*DRB*002:nov:01;DRB1*0302*
15, 17	*DRB*014:nov:01* *DRB*015:nov:01*
4, 9	*DRB*004:nov:01;DRB*W303*
8*	*DRB*005:nov:01* *DRB*006:nov:01*
5, 6, 19	*DRB*001:nov:02;DRB*W102* *DRB*008:nov:01*
10	*DRB*009:nov:01;DRB1*0302*
12	*DRB*009:nov:02*
18	*DRB*010:nov:01;DRB1*1002*
7	*DRB*011:nov:01* *DRB*012:nov:01*
8	*DRB*013:nov:01*
1	*DRB*016:nov:01;DRB1*W1001* *DRB*017:nov:01;DRB*W401*

Haplogroups 1 and 17 had a statistically suggestive association with JME affected status (Fig 8). We subsequently used RNA sequencing (RNAseq) to identify expressed MHC alleles within the 24 haplogroups, focusing on the Class II DRB locus due to its connection to MS in humans. RNAseq from 26 individuals provided data on 15 of the 24 haplogroups (Table 1). Eleven new Mafu-DRB alleles were identified and 7 previously found Mafu DRB alleles were extended. This analysis also showed that there are some allele expression differences within some haplogroups (8, 15/17), which suggests this higher resolution analysis will be important for the identification of haplotype associations with JME. Suggestive associations currently include *DRB* 014, DRB*015, DRB*016* and *DRB*017*, although additional studies, with additional individuals and full MHC expression analysis will be necessary to confirm potential association.

Analysis IL7R and IL2RA polymorphisms

Though their etiological fraction is far less than that of the MHC locus, several variants in the interleukin-7 receptor (IL7R) gene and interleukin 2 receptor-alpha (IL2RA) gene are reported to be associated with MS. To examine if these reported single base polymorphisms (SNPs) also occur in Japanese macaques, and whether they are associated with JME disease, we PCR amplified target regions of these genes to sequence in 38 animals of known phenotype (Table 2). The study set included 17 JME affected animals, 9 MRI+ animals, and 11 unaffected animals with no evidence for brain lesions by MRI analysis (MRI-). The gene regions targeted included: the promoters of both

genes, the CNS-1 regulatory region of IL7R, exons 2, 4, 6, and 8 of IL7R along with flanking intronic sequences.

Table 2. Allele frequencies for discovered SNP variants in Japanese macaques.

		IL7R Promoter SNP					IL7R - SNP *							IL2RA SNP	
	Allele	1	2	3	4	5	INT2-1	EX4-1	INT6-1	INT7-1	EX8-1	EX8-2	EX8-3	promoter 1	intron 1 rs2104286 #
JME affected n=17	Major	0.97	0.50	0.93	0.93	0.91	0.86	0.97	0.94	0.97	0.97	0.97	1.00	0.90	0.93
	Minor	0.03	0.50	0.07	0.07	0.08	0.14	0.03	0.06	0.03	0.03	0.03	0.00	0.10	0.07
MRI+ n=9	Major	1.00	0.44	0.88	1.00	0.88	1.00	1.00	1.00	1.00	1.00	1.00	1.00	0.88	0.94
	Minor	0.00	0.56	0.12	0.00	0.12	0.00	0.00	0.00	0.00	0.00	0.00	0.00	0.12	0.06
MRI- n=11	Major	0.86	0.59	0.95	0.91	0.95	0.95	0.95	0.91	0.95	0.95	0.95	1.00	0.91	0.91
	Minor	0.14	0.31	0.05	0.09	0.05	0.05	0.05	0.09	0.05	0.05	0.05	0.00	0.09	0.09
	Major	A	G	G	T	T	T	A	C	G	A	A	T	G	G
	Minor	T	C	A	C	C	C	G	A	A	T	G	C	C	A

* IL7R SNPs that occur within the exon are designed with EX before the exon number; SNPs that occur in an intron are designated with INT.

rs2104286 SNP reported in human sequence

One of the SNPs reported as associated with human MS, rs2104286, was also polymorphic in the Japanese macaques. Using the Fisher's exact test, we did not identify any significant associations between SNP alleles and either spontaneous JME or MRI+ status in this study set.

Additional findings

Pedigree analysis of all confirmed spontaneous JME cases was used to identify all first degree relatives amongst the full Japanese macaque colony. Using these data, it was shown that 1st degree relatives produced a more robust response to JMRV viral challenge than did non-related individuals (see Wong).

To expedite the discovery of sequence variants in JME candidate genes, we used exon-capture and next generation sequencing techniques to identify DNA polymorphisms in the exons and flanking regions of five JME 1st degree relative and 5 control animal genomes. Sequence was recovered in 90% of all coding sequences, providing a rich data set for the efficient, targeted analysis of additional candidate genes in the future.

Overall Aim 2 conclusions and future plans

Genetic risk factors that underlie the macaque demyelinating disease share at least two key parallels with human MS. First, JME risk is correlated with degree of kinship. Incidence of spontaneous disease has been documented in only 6 of 11 matrilines of ONPRC macaques, and first-degree relatives of JME cases have shown a more robust inflammatory response following intracranial infection of JMRV than those without a family history of JME. Second, the HLA alleles of the MHC locus provide the most consistent and compelling genetic risk factors for MS, and similarly in Japanese macaques, specific MHC alleles suggest an association with JME susceptibility. In contrast to humans, we found no variants in the IL7R or IL2RA genes that were significantly correlated with macaque demyelinating disease phenotype, although the study size was limiting. We conclude from these studies that JME disease risk mirrors MS disease risk in that it is likely the result of complex interactions of both genetic and environmental factors. We will continue to collect tissue from all new spontaneous JME cases for use in future genetic analyses, enabling improved refinement of the Japanese macaque MHC allele and increased power for testing candidate gene association with JME.

Task 3: To test the hypothesis that JMRV infection of glial cells directly influences demyelination and remyelination failure.

One of the original goals of this aim was to grow neurons and glia derived from Japanese macaque embryonic stem cells and test the effects of JMRV infection on cellular behaviors. However, we found that the neural stem cells derived from JM embryonic stem cells did not reliably give rise to each of the cell types we hoped to analyze (e.g. we observed neuronal differentiation but little or no oligodendrocyte progenitors or astrocytes). We therefore turned to acutely dissociated cultures of fetal cerebral cortex. We dissociated late term fetal temporal lobe cortex in trypsin-EDTA then grew cells in medium that we previously used to grow mouse neural progenitor cells (Matsuomoto et al., 2006). Under these culture conditions, we observed a mixture of cell types (Fig. 9) including $GFAP^+$ astrocytes, $map2^+$ neurons, and numerous $olig2^+$ oligodendrocyte progenitors. We also observed small numbers (<5% of the total population) of microglia, detected with the anti-IBA1 antibody as above (data not shown). We also observed small neurospheres growing in these cultures that could be propagated and which can differentiate into neurons, oligodendrocytes and astrocytes for >5 passages.

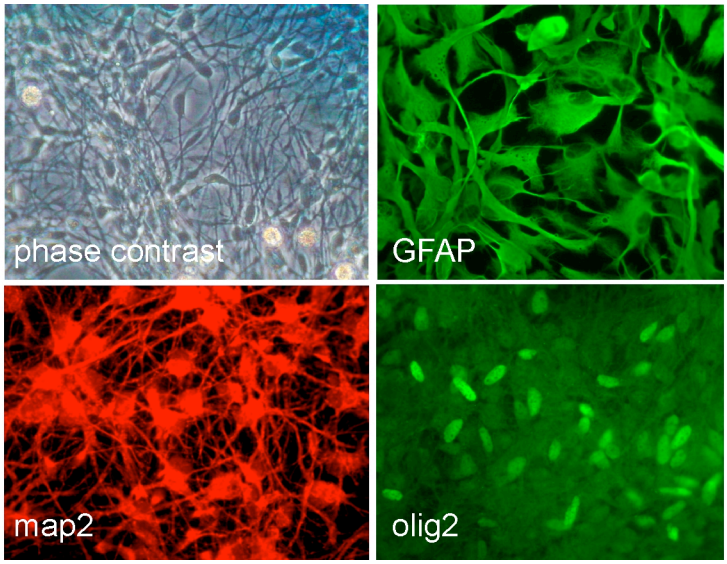

Figure 9. Microphotographs of acutely dissociated cultures of fetal Japanese macaque cortical cells. Cultures were grown on poly-l-lysine coated glass coverslips in a mixture of DMEM/F12 medium supplemented as previously described by us (Matsumoto et al., 2006) then processed for immunocytochemistry. GFAP = glial fibrillary acidic protein, a marker of atrocities; map2 = microtubule associated protein, a marker of neurons; olig2 = a marker of oligodendrocyte progenitor cells.

Using these cultures, we have found that JMRV infects microglia and oligodendrocyte lineage cells, as well as neurons. We did not find substantial levels of infection in astrocytes. This is consistent with our findings in tissues from infected animals (e.g. Fig. 2C and data not shown). Furthermore, we found that JMRV infection caused significant cell death in cultures.

KEY RESEARCH ACCOMPLISHMENTS

To date, we have accomplished the vast majority of the original goals of this grant. In particular, we have:

1. Demonstrated that intracranial infection with JMRV in animals from affected lineages, but not from unaffected lineages is sufficient to induce disease
2. Demonstrated that genetic variations in particular MHC haplotypes are associated with disease susceptibility
3. Demonstrated that JMRV infects glial cells (including microglia) and neurons, and can induce cell death
4. Demonstrated that JME lesions resemble MS lesions with regards to demyelination, axon damage, and the accumulation of hyaluronan.

REPORTABLE OUTCOMES

We have three manuscripts in preparation describing (a) our findings demonstrating that JMRV can induce inflammatory demyelination and axonopathy in susceptible animals; (b) that chronic JME lesions persists in some animals well after initial attacks; and (c) that specific MHC haplotypes are linked to disease susceptibility. A manuscript characterizing JME for the first time was published in *Annals of Neurology* in 2011 (see appendix).

CONCLUSION

We have characterized an encephalomyelitis in Japanese macaques whose hallmarks are motor and sensory deficits; T and B cell infiltration into the brain and spinal cord; and CNS demyelination and axonopathy. The disease only occurs in animals belonging to specific families, and is associated with the presence of specific HLA alleles of MHC. We have demonstrated that the disease is triggered in animals from affected lineages by a virus (JMRV) that appears to be unique to the colony at ONPRC. We have found that this virus infects microglia as well as oligodendrocytes and neurons and is sufficient to trigger an autoimmune response following intracranial injection. All together, these data support our hypothesis that JME is similar in both etiology and pathology to MS, and that JME may serve as a unique and unprecedented model for inflammatory demyelinating diseases like MS.

This new model is significant for a number of reasons. Numerous clinical trials that were designed directly from rodent studies alone have failed, in large part because rodent and human physiology, anatomy and genetics are so different. The Japanese macaque more closely resembles humans and offers investigators conducting pre-clinical trials the opportunity to perform safety and efficacy studies that better inform human clinical trials than rodent studies. This model also offers a unique opportunity to better understand early events in disease onset, since we are able to selectively induce the disease by infecting genetically liable animals. Finally, this model offers the unprecedented opportunity to investigate how genetic variations in MHC loci contribute to disease susceptibility, onset and progression.

We have requested a no-cost extension to complete these studies (increasing the sample size for the final studies using infected animals) and will publish our findings in the next year. We hope the leverage the funds that supported this project to obtain additional funds for our studies with the long-term aim of using this model to better understand how MS and other inflammatory demyelinating diseases can be treated and possibly prevented.

REFERENCES

Ascherio A, Munger KL. Epstein-barr virus infection and multiple sclerosis: a review. J Neuroimmune Pharmacol. 2010 Sep;5(3):271-7.

Axthelm MK, Bourdette DN, Marracci GH, Su W, Mullaney ET, Manoharan M, Kohama SG, Pollaro J, Witkowski E, Wang P, Rooney WD, Sherman LS, Wong SW. Japanese macaque encephalomyelitis: a spontaneous multiple sclerosis-like disease in a nonhuman primate. Ann Neurol. 2011 Sep;70(3):362-73.

Back SA, Tuohy TM, Chen H, Wallingford N, Craig A, Struve J, Luo NL, Banine F, Liu Y, Chang A, Trapp BD, Bebo BF Jr, Rao MS, Sherman LS. Hyaluronan accumulates in demyelinated lesions and inhibits oligodendrocyte progenitor maturation. Nat Med. 2005 Sep;11(9):966-72.

Du YP, Chu R, Hwang D, Brown MS, Kleinschmidt-DeMasters BK, Singel D, Simon JH. Fast multislice mapping of the myelin water fraction using multicompartment analysis of T2* decay at 3T: a preliminary postmortem study. Magn Reson Med. 2007;58:865-70.

Harley JB. IL-7Ralpha and multiple sclerosis risk. Nat Genet. 2007 Sep;39(9):1053-4.

Labadie C, Rooney WD, Springer CS, Lee J-H, Aubert-Frécon M, Hetzer S, Mildner T, and Möller HE. Observation of myelin water at ultra short echo time by longitudinal relaxographic imaging with spin-echo echo-center-out-EPI (DEPICTING). Proc. Int. Soc. Magn. Reson. Med. 19, 230 (2011).

Levin LI, Munger KL, O'Reilly EJ, Falk KI, Ascherio A. Primary infection with the Epstein-Barr virus and risk of multiple sclerosis. Ann Neurol. 2010 Jun;67(6):824-30.

Matsumoto S, Banine F, Struve J, Xing R, Adams C, Liu Y, Metzger D, Chambon P, Rao MS, Sherman LS. Brg1 is required for murine neural stem cell maintenance and gliogenesis. Dev Biol. 2006 Jan 15;289(2):372-83.

Ramagopalan SV, Knight JC, Ebers GC. Multiple sclerosis and the major histocompatibility complex. Curr Opin Neurol. 2009 Jun;22(3):219-25.

van Gelderen P, de Zwart JA, Lee J, Sati P, Reich DS, Duyn JH. Nonexponential T(2) * decay in white matter. Magn Reson Med. 2012;67:110-7.

APPENDIX

Axthelm MK, Bourdette DN, Marracci GH, Su W, Mullaney ET, Manoharan M, Kohama SG, Pollaro J, Witkowski E, Wang P, Rooney WD, Sherman LS, Wong SW. Japanese macaque encephalomyelitis: a spontaneous multiple sclerosis-like disease in a nonhuman primate. Ann Neurol. 2011 Sep;70(3):362-73. doi: 10.1002/ana.22449. Epub 2011 Jun 14. PMID: 21674589

Japanese Macaque Encephalomyelitis: A Spontaneous Multiple Sclerosis–like Disease in a Nonhuman Primate

Michael K. Axthelm, DVM, PhD,[1,2] Dennis N. Bourdette, MD,[3] Gail H. Marracci, PhD,[3] Weiping Su, PhD,[4] Elizabeth T. Mullaney, BS,[2] Minsha Manoharan, MS,[2] Steven G. Kohama, PhD,[4] Jim Pollaro, MS,[5] Ellen Witkowski, BA,[4] Paul Wang, MD,[5] William D. Rooney, PhD,[5] Lawrence S. Sherman, PhD,[4] and Scott W. Wong, PhD[1,2,6]

Objective: To describe Japanese macaque encephalomyelitis (JME), a spontaneous inflammatory demyelinating disease occurring in the Oregon National Primate Research Center's (ONPRC) colony of Japanese macaques (JMs, *Macaca fuscata*).
Methods: JMs with neurologic impairment were removed from the colony, evaluated, and treated with supportive care. Animals were humanely euthanized and their central nervous systems (CNSs) were examined.
Results: ONPRC's JM colony was established in 1965 and no cases of JME occurred until 1986. Since 1986, 57 JMs spontaneously developed a disease characterized clinically by paresis of 1 or more limbs, ataxia, or ocular motor paresis. Most animals were humanely euthanized during their initial episode. Three recovered, later relapsed, and were then euthanized. There was no gender predilection and the median age for disease was 4 years. Magnetic resonance imaging of 8 cases of JME revealed multiple gadolinium-enhancing T_1-weighted hyperintensities in the white matter of the cerebral hemispheres, brainstem, cerebellum, and cervical spinal cord. The CNS of monkeys with JME contained multifocal plaque-like demyelinated lesions of varying ages, including acute and chronic, active demyelinating lesions with macrophages and lymphocytic periventricular infiltrates, and chronic, inactive demyelinated lesions. A previously undescribed gamma-herpesvirus was cultured from acute JME white matter lesions. Cases of JME continue to affect 1% to 3% of the ONPRC colony per year.
Interpretation: JME is a unique spontaneous disease in a nonhuman primate that has similarities with multiple sclerosis (MS) and is associated with a novel simian herpesvirus. Elucidating the pathogenesis of JME may shed new light on MS and other human demyelinating diseases.

ANN NEUROL 2011;70:362–373

Multiple sclerosis (MS) is a chronic inflammatory disease that affects the central nervous system (CNS). The disease typically follows a relapsing-remitting course and is associated with a variety of neurological deficits, such as paralysis, imbalance, ataxia, blindness, and ocular motor paresis (reviewed in Noseworthy and colleagues[1]). Classically, the pathology of MS consists of discrete, multifocal areas of demyelination, associated with variable axonal loss in the white matter of the brain, spinal cord and optic nerves. More recently, lesions within the gray matter have been described. Lesions with active demyelination are associated with infiltrating lymphocytes and lipid-laden phagocytic macrophages. Although the cause of MS remains uncertain, there is considerable evidence indicating that multiple genetic loci and incompletely understood environmental exposures influence the risk of developing MS (reviewed in Libbey and colleagues[2]). One still unproven hypothesis is that a viral infection occurring in genetically susceptible individuals induces the disease.

The most widely studied model of MS is experimental autoimmune encephalomyelitis (EAE) (reviewed

View this article online at wileyonlinelibrary.com. DOI: 10.1002/ana.22449

Received Dec 15, 2010, and in revised form Mar 23, 2011. Accepted for publication Apr 1, 2011.

Address correspondence to Dr Wong, PhD, Vaccine and Gene Therapy Institute, 505 NW 185th Avenue, Beaverton, OR 97006. E-mail: wongs@ohsu.edu

From the [1]Division of Pathobiology and Immunology and [4]Division of Neuroscience, Oregon National Primate Research Center, Beaverton, OR; [2]Vaccine and Gene Therapy Institute, Oregon Health and Science University, Beaverton, OR; [3]Neurology and Research Service, Department of Veterans Affairs Medical Center and Department of Neurology, [5]Advanced Imaging Research Center, and [6]Department of Molecular Microbiology and Immunology, Oregon Health and Science University, Portland, OR.

in Libbey and colleagues[3]). This paralytic illness can be induced in a variety of mammalian species by immunization with whole myelin or specific myelin proteins, most notably myelin basic protein (MBP), myelin oligodendrocyte glycoprotein, and proteolipid protein, or peptides from these proteins.[4–6] Depending on the species used and method of disease induction, EAE can follow a chronic relapsing course and be associated with multifocal areas of demyelination and thus mimic MS pathologically and clinically.[7] There are also mouse models of virally induced demyelinating diseases, most notably Theiler's murine encephalomyelitis virus (TMEV).[8–10] TMEV-induced demyelinating disease (TMEV-IDD) is induced by injecting neurotropic strains of the virus into genetically susceptible mice.[11] Depending upon the strain of TMEV, infection can result in either acute encephalitis or a chronic immune-mediated multifocal demyelinating disease. While EAE can be induced in rhesus and common marmoset monkeys, a virally induced model of MS has not been described in nonhuman primates (NHPs). Availability of a demyelinating disease associated with a virus in an NHP might prove relevant to understanding the pathogenesis of MS.

Here, we report the spontaneous occurrence of an inflammatory demyelinating disease in a colony of Japanese macaques (JMs, *Macaca fuscata*) at the Oregon National Primate Research Center (ONPRC). The disease, Japanese macaque encephalomyelitis (JME), has clinical and pathologic similarities with MS. Moreover, we report the isolation of a previously undescribed simian herpesvirus isolated from acute JME lesions. This is the first description of a spontaneously occurring MS-like disease in an NHP and has the potential to offer new insights into the pathogenesis of MS.

Subjects and Methods

Animals

All animal procedures were approved by the ONPRC Institutional Animal Care and Use Committee. The ONPRC is an Association for Assessment and Accreditation of Laboratory Animal Care International accredited research facility and conforms to National Institutes of Health guidelines on the ethical use of animals in research. The JM colony is maintained in a 2-acre corral and members of the colony are observed daily for the presence of sick or injured animals. Per institutional protocol, members of the colony developing neurologic dysfunction were removed from the corral, placed in cages, evaluated, and provided supportive care. Most animals developing JME were humanely euthanized per ONPRC protocol. Three animals recovered from their initial episode and were returned to the corral, but later relapsed and were then humanely euthanized.

Clinical Sample Analysis

Cerebrospinal fluid (CSF) was acquired from sedated animals and analyzed for total protein, cell count, and cell type determination. Complete blood count and routine serum chemistries were obtained.

Histopathological Examination

Complete necropsies were performed on all animals. CNS tissues were collected from most animals and either placed in neutral-buffered formalin or neutral-buffered 4% paraformaldehyde for paraffin embedding or media for isolation of a potential infectious agent. Sections from the CNS were cut at 5μm, deparaffinized, and stained with hematoxylin and eosin, Luxol fast blue–periodic acid-Schiff (PAS)–hematoxylin stain, or Bielschowsky's silver impregnation to image axons, or blocked with 5% normal goat serum and 5% bovine serum albumin for immunostaining with primary antibodies specific for MBP (rabbit anti-MBP, Zymed, San Francisco, CA; 1:100), neurofilament (NF) light chain (mouse anti-NF, Chemicon, Temecula, CA; 1:500), oligodendrocytes lineage transcription factor 2 (olig2) (rabbit anti-olig2, Chemicon; 1:500), T cells (rabbit anti-CD3, Dako; 1:200), or macrophages (mouse anti-CD68, Dako, Carpinteria, CA; 1:80). Secondary antibodies used were as follows: goat-anti-rabbit immunoglobulin G (IgG) conjugated to Alexa 488 (Molecular Probes, Eugene, OR; 1:500), goat-anti-mouse IgG conjugated to Alexa 546 (Molecular Probes; 1:500), biotinylated goat-anti-rabbit IgG and biotinylated goat-anti-mouse IgG. Streptavidin-Alexa 488 and Streptavidin-Alexa 594 were utilized to visualize CD3+ T cells and CD68+ macrophages, respectively. The sections were then counterstained with 4,6′-diamino-2-phenylindole dihydrochloride (DAPI) (1:5,000) and analyzed by light or fluorescent microscopy performed on a Zeiss (Gottingen, Germany) microscope equipped with an Axiocam digital camera.

For quantitation of olig2-immunolabeled cells, 3 adjacent sections were analyzed at ×40 following double labeling with anti-MBP and anti-olig2 antibodies. Three regions of interest (ROIs) were identified using MBP labeling: the lesion, where MBP immunoreactivity was mostly absent; the border, where there was a mixture of intact myelin and damaged myelin; and adjacent unaffected white matter. The number of olig2+ cells in 3 random microscopic fields within each ROI in each adjacent section was then counted and averaged. The mean differences between ROIs were assessed using Student *t* test.

Magnetic Resonance Imaging

A 4-year 240-day-old female JM exhibiting signs of JME was transported to Oregon Health and Science University Hospital, anesthetized and positioned in a General Electric (Waukesha, WI) 1.5T Signa magnetic resonance imaging (MRI) instrument and T_2-weighted and pregadolinium and postgadolinium T_1-weighted images were obtained from the brain and cervical cord. All other MRIs were performed on a 3T Siemens (Erlangen, Germany) Trio whole-body MRI instrument using a quadrature transmit/receive extremity radiofrequency coil. Sixty sagittally-oriented 2-dimensional (2D) turbo spin echo acquisitions

with proton density (echo time [TE] = 17msec/recycle time [TR] = 9000msec/echo train length [ETL] = 9/number of excitations [NEX] = 1) contrast were collected with a 1mm slice thickness using a 256 × 256 matrix over a 160mm^2 field-of-view (FOV). Multislice 2D turbo spin echo MRI acquisitions with proton density (TE = 13msec/TR= 9000msec/ETL= 9msec/NEX = 2) and T_2-weighted (TE= 92msec/TR = 9000msec/ETL = 9/NEX = 2) contrast were collected in an axial orientation angulated parallel to the imaginary line connecting the anterior and posterior commissures; 66 1mm slices were collected using a 320 × 240 matrix over a 160mm × 120mm FOV. Transaxial 3D T_1-weighted magnetization prepared rapid acquisition gradient echo (MPRAGE); TE = 3.5msec/TR = 2500msec/inversion time [TI] = 900msec/flip angle [FA] = 8) data sets were acquired before and 30 minutes after gadoteridol administration with a 192 × 144 × 96 matrix over a 130mm × 98mm × 76mm FOV. Gadoteridol was administered in situ at a dose of 0.2mmol/kg using an infusion pump.

Isolation of a Herpesvirus from an Acute Lesion

A spinal lesion from a JM (#17792) with JME was obtained at necropsy, homogenized, and placed over primary rhesus macaque fibroblasts for isolation and analysis of a potential infectious agent as described.[12] Preliminary molecular characterization to identify the herpesvirus was conducted as described.[12] Using the same technique, attempts were made to isolate viruses from other acute JME lesions and normal white matter from JM with and without JME.

Results

JME

The ONPRC has housed an outbred colony of JMs since 1965. No cases of unexplained neurologic disease were observed in the colony prior to 1986. Since 1986, 56 JMs spontaneously developed JME (Fig 1). Currently, 1% to 3% of the colony develops JME each year and the disease affects males and females equally. Except for the burst of cases in August 1987, there is no apparent seasonal predilection and cases have occurred every year since 1986 except in 1993 and 2004. Table 1 provides details of the clinical features of the disease on the 56 cases. The median age of affected animals was 4 years 109 days (range, 97 days–26 years 50 days). The majority of the animals had paresis or paralysis of 1 or more limbs and ataxia. Ocular paresis occurred in 10 cases. Seven animals exhibited other clinical manifestations, including abnormal species-specific behaviors and head tilt accompanied with body tremors. Typically, the onset of clinical disease was acute and progressed rapidly with the median time between presentation of disease to humane euthanasia being 6 days (range, 0 days–121 days). In most cases, euthanasia was required because neurologic impairment made it impossible to return the monkeys safely to the colony. Three animals (#12068, 21255, and 16749) recovered from their initial episode and were returned to the corral, but were later euthanized when their JME recurred 101 days to 8 years later.

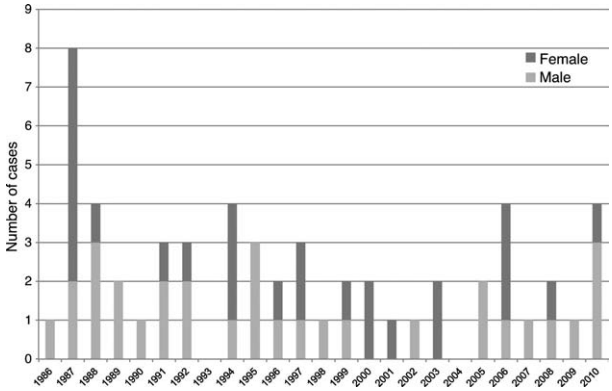

FIGURE 1: Number of Japanese macaques affected each year with Japanese macaque encephalomyelitis.

CSF was collected from 40 affected animals. The mean CSF white blood cell (WBC) count was 185 cells/mm^3 with a range from 0 to 2,710. WBC differential was obtained in 13 cases and in all but 1 the cells consisted of both lymphocytes and neutrophils. The mean total protein was 52mg/dl (range, 0–195mg/dl). Glucose values were normal and attempts to isolate bacteria from CSF were negative. Hematological and biochemical examinations of blood revealed no consistent abnormalities. CSF was not examined for oligoclonal bands or IgG index.

MRI Abnormalities

MRI scans were performed on 8 animals with JME and MRI scans from 3 cases are shown in Figure 2. A brain and cervical MRI scan was performed on JM #19384 11 days after presentation with clinical signs of JME (see Fig 2A–C). Postgadolinium T_1-weighted images revealed multiple areas of focal contrast enhancement in the white matter of the cerebral hemispheres, cerebellum, brainstem, and cervical spinal cord. JM #26174 underwent MRI 4 days after presentation with acute JME signs (see Fig. 2D–I). The T_2-weighted axial images in Figure 2D–F showed hyperintense areas in the upper cervical spinal cord, cerebellum, and cerebrum. The axial images of Figure 2G–I show intense focal contrast enhancement in the upper cervical spinal cord, cerebellum, and genu of the corpus callosum. JM #13221 underwent MRI 1 day after presentation with acute JME symptoms (see Fig 2J–L). T_2-weighted axial images revealed a large hyperintense area in the left cerebral peduncle (see Fig 2J). The same area had a hypointense appearance in the T_1-weighted MPRAGE image (see Fig 2K). Punctate gadolinium enhancement was apparent in this same peduncle region in the postcontrast T_1-weighted image (see Fig 2L). The

TABLE 1: Clinical Findings in Cases of JME*

ID#	Sex	Age at Onset (yr/day)	Duration of Disease Prior to Euthanasia (days)	Paresis	Ataxia	Optical	Other	CSF Cells/mm^3 (% lymphocyte/ neutrophil)	CSF Protein (mg/dl)
13762	M	1Y76D	6	X				1 (ND)	20
03246	F	20Y17D	61				X		
14871	F	0Y94D	3		X			336 (ND)	0
12800	X[a]	4Y95D	14	X	X	X		186 (ND)	107
14528	X[a]	1Y46D	52		X	X			
14873	M	0Y164D	4			X			
13754	M	2Y104D	2				X	2,710 (ND)	112
07804	F	12Y116D	14		X	X		58 (ND)	0
09179	F	10Y136D	83	X				0 (ND)	11
08234	F	12Y112D	20	X		X		11 (ND)	104
14214	M	2Y64D	0				X		
15535	M	0Y123D	3				X		
13998	M	3Y122D	13		X				
08420	M	13Y19D	4		X			30 (ND)	113
13752	M	3Y336D	3		X				
12113	M	7Y325D	22		X			0 (ND)	22
13768	F	6Y259D	2	X		X		112 (ND)	50
15997	M	1Y336D	1	X				83 (ND)	71
16376	M	0Y327D	2		X			204 (ND)	29
16387	M	1Y235D	7	X				70 (ND)	48
13744	X[a]	7Y185D	6		X			8 (ND)	12
13993	M	6Y337D	0				X		
15306	M	5Y272D	5	X	X	X		12 (ND)	195
12817	F	11Y31D	13	X				20 (ND)	29
11032	F	14Y133D	6				X	68 (ND)	16
12059	F	12Y251D	3		X			10 (ND)	70
17792	M	1Y258D	5	X				385 (ND)	86
16777	M	3Y354D	20		X	X		2 (ND)	10
12068[b]	M	13Y86D	4	X				174 (ND)	16
18247	M	1Y245D	16	X		X		87 (ND)	39
18925	F	0Y197D	7	X				22 (ND)	21
19325	M	0Y250D	2	X					
19085	F	1Y111D	49	X				58 (ND)	17
19395	F	0Y305D	1		X	X			
16746	F	7Y125D	5	X				20 (ND)	37

TABLE 1 (Continued)

ID#	Sex	Age at Onset (yr/day)	Duration of Disease Prior to Euthanasia (days)	Paresis	Ataxia	Optical	Other	CSF Cells/mm^3 (% lymphocyte/ neutrophil)	CSF Protein (mg/dl)
19894	M	1Y220D	0	X					
20472	F	0Y291D	0	X				108 (ND)	50
19400	F	3Y210D	19	X				541 (ND)	144
19384	F	4Y188D	53	X				88 (10/90)	103
16749[c]	F	9Y259D	124		X			56 (75/25)	21
12812	M	18Y207D	10	X				60 (86/14)	104
22699	F	1Y212D	6	X				230 (26/74)	55
22007	F	2Y351D	13	X				353 (92/8)	63
24059	M	1Y303D	3	X				408 (68/32)	0
24043	M	2Y180D	1	X					
24631	F	1Y225D	5	X					
22720	F	4Y203D	13	X				3 (100)	6
21282	F	6Y359D	32	X				9 (20/80)	7
18270	M	12Y38D	6	X				70 (25/75)	15
21255[d]	M	8Y93D	0	X					
26174	M	2Y225D	4	X				650 (25/75)	168
27616	F	0Y217D	1	X				123 (61/39)	55
18276	M	14Y321D	6		X				
20482	M	11Y304D	13		X			37 (71/29)	14
28422	M	0Y276D	6				X	11 (80/20)	25
13221	X[a]	26Y49D	1		X				

*The clinical presentation of JMs with JME is similar to MS. Ataxia, paralysis or paresis of one or more limbs, and ocular abnormalities clinically characterizes JME.
[a]X refers to a female pseudohermaphroditic animal.
[b]Animal 12068 had an initial episode of JME at 5 years 281 days and a second episode at 13 years 90 days.
[c]Animal 16749 had an initial episode at 9 years 212 days and a second episode at 10 years 18 days.
[d]Animal 21255 had an initial episode at 341 days and a second episode at 8 years 93 days.CSF = cerebrospinal fluid; JM = Japanese macaque; JME = Japanese macaque encephalomyelitis; MS = multiple sclerosis; ND = no data.

MRI abnormalities displayed here are similar to those of the other 5 cases of JME that underwent MRI, consistent with active neuroinflammation and similar to the MRI findings of acute lesions in MS.

Neuropathology

Complete necropsies were performed on 54 of 56 cases of JME. No monkeys had evidence of a systemic illness or acute disease outside of the CNS. In all cases, neuropathologic examination of the brain and cervical spinal cord revealed a multifocal demyelinating encephalomyelitis. In most cases, multiple, dull, yellow-white to gray-tan, well-delineated plaques that ranged from 0.2 to 1.0cm in greatest dimension were apparent on gross inspection of postfixed coronal brain and spinal cord slices. Gross lesions were most frequent in the cerebellar white matter, brachium pontis, pyramids, and the white matter of the cervical spinal cord. A typical distribution of plaque-like lesions in the cerebellum and spinal cord was found in animal #19384 that underwent MRI (Fig 3A). Histologically, a majority of lesions seen in all JME cases had morphologic features consistent with the

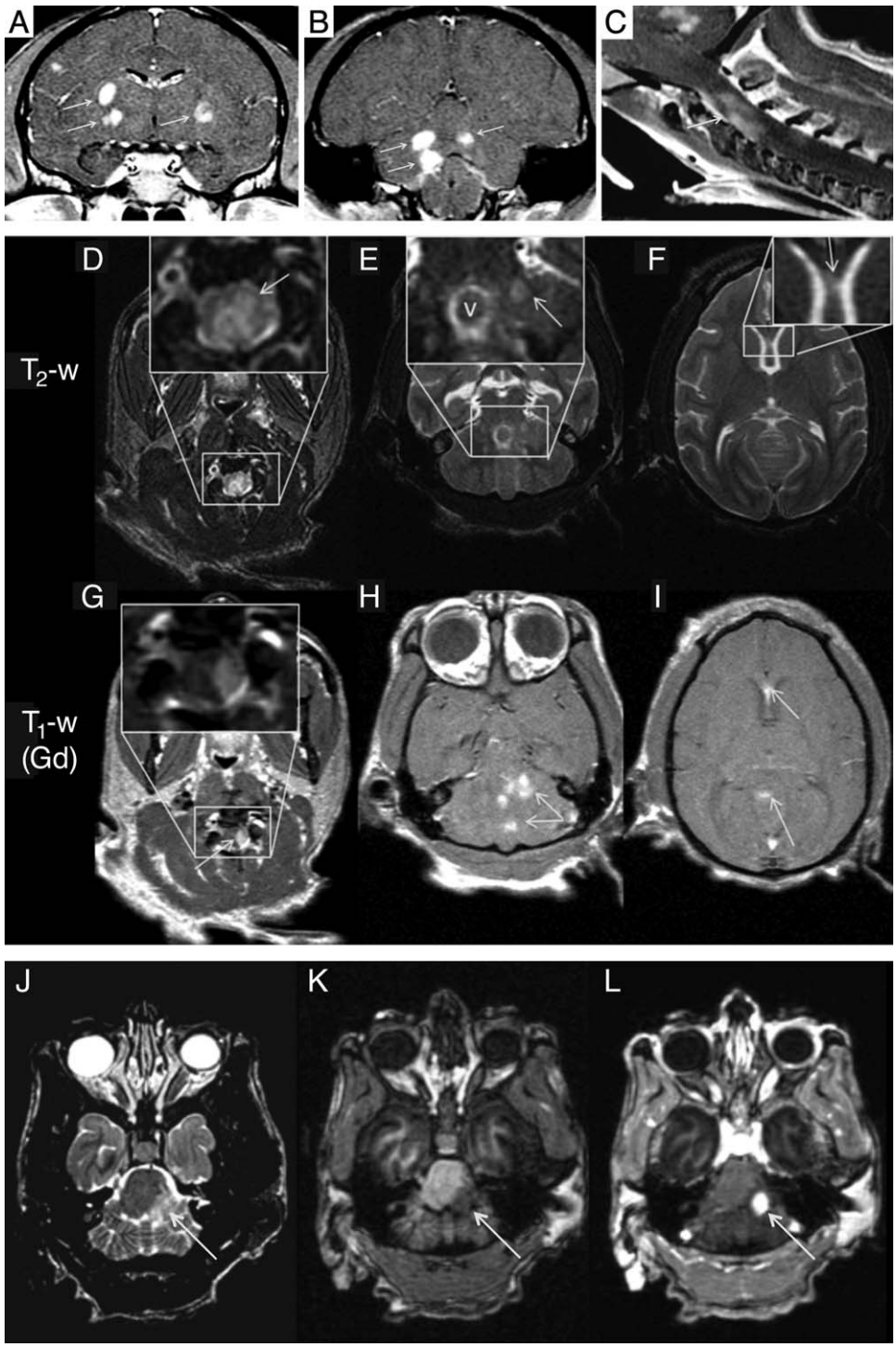

FIGURE 2: MRI of animals with JME. (A–C) Postgadolinium T_1-weighted MRI images from JM #19384 11 days after presentation with acute flaccid paralysis of the right pelvic limb. (A) Coronal image of cerebral hemispheres reveals gadolinium-enhanced lesions *(arrows)* in the internal capsule. (B) Coronal image of posterior cerebral hemispheres, cerebellum, and brainstem shows 3 gadolinium-enhanced lesions in corpus medullare *(arrows)* of the cerebellum. (C) Sagittal image of upper cervical cord shows gadolinium-enhanced lesion *(arrow)*. (D–I) Axial 3T MRI images from JM #26174 obtained 4 days after developing signs of JME. (D) Axial T_2-weighed image of upper cervical spinal cord shows hyperintense signal that is expanded in insert and identified *(arrow)*. (E) Hyperintense signal in cerebellar region that is expanded in insert and denoted *(arrow)*. The hyperintense ring surrounding "v" in the insert is CSF fluid superior to the 4th ventricle adjacent to the superior medullary velum. (F) Hyperintense signal in the genu of the corpus callosum that is expanded in the insert and identified *(arrow)*. Axial postgadolinium T_1-weighted image shows enhancing lesions in (G) upper cervical spinal cord, (H) cerebellum, and (I) genu of the corpus callosum. (J–L) Axial 3T MRI images from JM #13221 during the acute phase of JME. (J) Axial T_2-weighted image shows hyperintense lesion in the left lateral pons and peduncule *(arrow)* that is hypointense on a (K) T_1-weighted precontrast MPRAGE image *(arrow)*. (L) The lesion enhances on a T_1-weighted MPRAGE image acquired 30 minutes after the administration of 0.2mmol/kg gadoteridol *(arrow)*. CSF = cerebrospinal fluid; JM = Japanese macaque; JME = Japanese macaque encephalomyelitis; MPRAGE = magnetization prepared rapid acquisition gradient echo; MRI = magnetic resonance imaging.

chronic active plaques described in MS.[13–17] Plaques were typically centered on venules or small veins. The chronic active plaques (see Fig 3B) were dominated centrally by macrophages engorged with myelin debris intermingled with astrocytes. Infiltrating macrophages and lymphocytes dominated in peripheral portions of plaques with focal concentrations of lymphocytes forming perivascular cuffs. Areas of necrosis and microcystic spaces were occasionally observed in the central portion of chronic-active lesions. Variations in lesion age were observed in some animals. Early lesions were infrequent and characterized by perivenous lymphocytic cuffs that frequently tracked perforating venules from pia-arachnoid surfaces into adjacent white matter. The adjacent myelin was vesiculated and sparsely infiltrated with lymphocytes and macrophages. Rarely, small focal hemorrhages were encountered in the edematous myelin. Chronic inactive plaques composed principally of astrocytes and foamy macrophages were seen in many of the animals (see Fig 3C). Lymphocytes were largely absent in these lesions and silver staining revealed decreased numbers of axons with evidence of acute axotomies (see Fig 3D, E). Regardless of apparent age, lesions were exclusively located in white matter in all animals. Apart from rare, small, perivascular collections of lymphocytes, lesions were not seen in gray matter or the meninges. Transmission electron microscopy (EM) was performed on a limited number of lesions and these disclosed degenerating axons, demyelinated axons and occasional thinly myelinated axons, suggesting remyelination (data not shown).

Immunostaining was performed on 2 lesions localized by MRI in JM #13221. The first lesion was analyzed by immunostaining for alterations in MBP, NF, and olig2 immunoreactivity, and a second for infiltration of macrophages and T cells. MBP and NF labeling demonstrated areas with axon and myelin debris (defined as the demyelinated lesion) adjacent to border areas showing a mixture of intact and damaged fibers, which was,

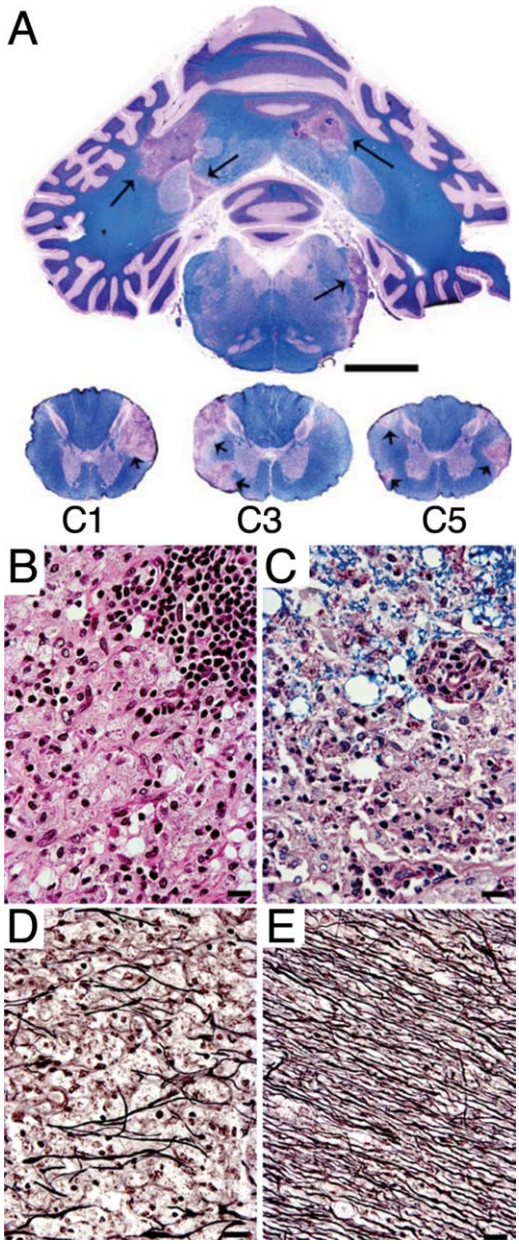

FIGURE 3: Histopathology of JME. Histopathological examination of the brain of JM #19384 obtained 53 days following clinical presentation of JME. (A) Luxol fast blue-PAS-hematoxylin stain of cerebellum and cervical spinal cord. Note the large, well-defined, irregular-shaped areas of myelin loss in the corpus medullare of the cerebellum *(arrows)* corresponding to the lesions seen 42 days earlier in the MRI images (see Fig 2B). Similar lesions are present in the lateral white matter columns of the 1st, 2nd, and 5th cervical spinal cord segments *(arrows)*; the abnormalities in the upper cervical cord correspond to lesions seen on MRI (see Fig 2C). Bar = 1cm. (B) High-power magnification of a portion of the large chronic active plaque in the upper left of the cerebellum. Normal appearance of white matter is obliterated by large foamy macrophages and scattered lymphocytes. Swollen myelin sheaths appear as circular, optically clear spaces. A portion of a thick perivascular lymphocytic cuff is present in the upper right of the panel. Hematoxylin-eosin stain; Bar = 50μm. (C) Portion of a chronic inactive plaque from the cerebellum. Note that the myelin in the upper portion of the panel is vesiculated but retains Luxol fast blue staining. Macrophages containing reddish PAS-stained debris and astrocytes obliterate normal white matter architecture in the bottom portion of the panel. Luxol fast blue-PAS-hematoxylin stain; Bar = 50μm. (D,E) Reduced number of axons in the center of (D) a chronic inactive plaque compared to (E) normal axonal density in normal appearing white matter. Bielschowsky's silver impregnation axonal stain; Bar = 50μm. JM = Japanese macaque; JME = Japanese macaque encephalomyelitis; MRI = magnetic resonance imaging; PAS = periodic acid-Schiff.

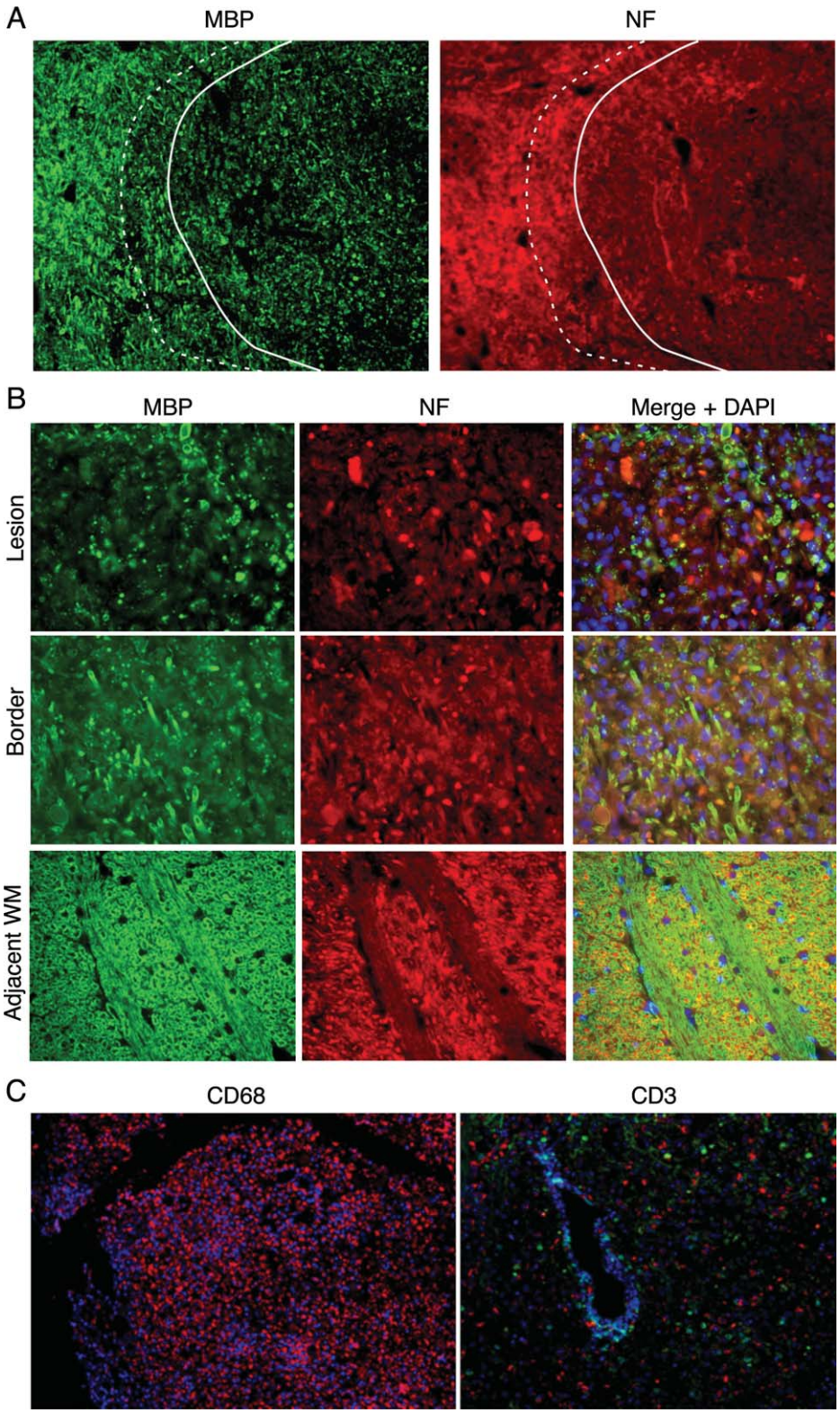

FIGURE 4: Demyelination and axonal loss in JME lesion. Immunofluorescent imaging from pontine lesion from JM #13221 identified by MRI (see Fig 2J–L). (A) The pontine lesion was double-labeled for MBP *(green)* and NF *(red)* to visualize demyelination and loss of neurons. Area to the right of the solid line demarcates demyelinated lesion and shows marked reduction in staining for MBP and NF, indicating loss of myelin and axons; dashed line is lesion border with mix of damaged myelin and normal appearing myelin. Area to the left of the dashed line is unaffected WM (×5 magnification). (B) High magnification images of the lesion, border, and unaffected white matter stained for the presence of MBP, NF, and DAPI for nuclei to visualize the extent of demyelination and axonal damage. Note reduction in MBP and NF staining in both the lesion and border areas. The merged image of lesion and border reveals increased cellularity (increased DAPI staining), some preserved myelinated axons and some NF+ axons without myelin. (×40 magnification). (C) A cerebellar lesion from JM #13221 showing CD68+ macrophages *(red)* and CD3+ T cells *(green)* near a venule *(blue)* (×10 and ×20 magnification, respectively). (D) The lesion site in A was immunostained for olig2 to assess the presence of oligodendrocytes and with a nuclear stain (DAPI) in the lesion, border, and unaffected WM. Note the reduction in staining in the sections from the lesion and border areas for olig2 with increased numbers of DAPI+ cells (×40 magnification). (E) Quantification of olig2 immunolabeling. Three adjacent sections were analyzed and 3 random fields in each section were counted at the lesion, lesion border, and in adjacent WM, showing significant reduction in olig2+ cells in the lesion and border compared with normal WM ($p < 0.01$). DAPI = 4,6′-Diamino-2-phenylindole dihydrochloride; JM = Japanese macaque; JME = Japanese macaque encephalomyelitis; MBP = myelin basic protein; MRI = magnetic resonance imaging; NF = neurofilament; WM = white matter.

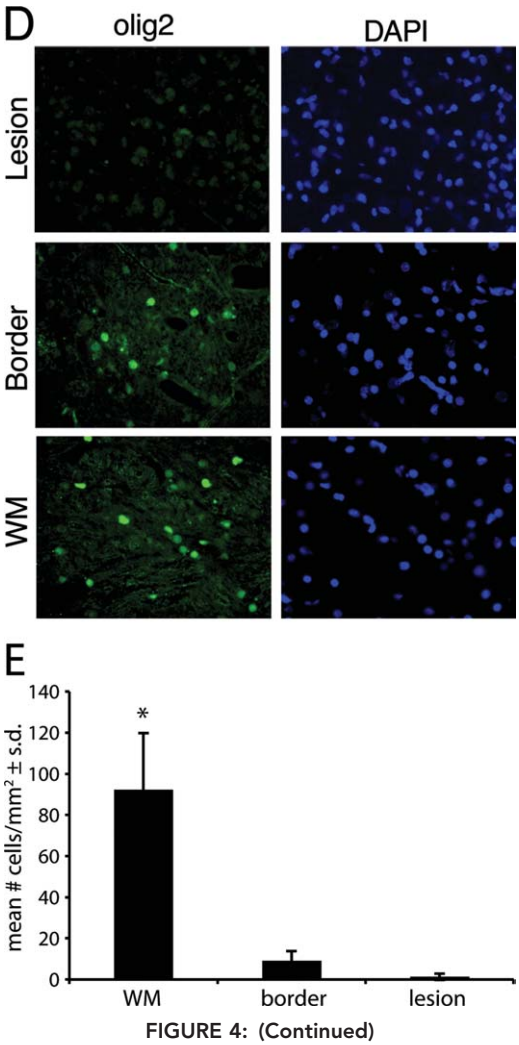

FIGURE 4: (Continued)

in turn, adjacent to unaffected white matter (Fig 4A, B). Staining for the presence of CD68 in a lesion located in the cerebellum revealed numerous CD68+ macrophages and perivascular CD3+ T cells (see Fig 4C). Oligodendrocytes were quantified by enumerating olig2-labeled cells within the lesion shown in Figure 4A and B. There was nearly complete absence of olig2 immunoreactivity within the lesion and a dramatic reduction in olig2+ cells at the lesion border compared to adjacent unaffected white matter (see Fig 4D, E). The lesions of JME thus are multifocal, contain T cell and macrophage infiltrates, and reveal demyelination, loss of oligodendrocytes, limited remyelination, and axonal degeneration.

Isolation of Novel Gamma-2 Herpesvirus from Encephalomyelitis Lesions

As viral infection has been associated with inflammatory demyelination in mice, we investigated whether a virus might be present in acute lesions of animals with JME. Explant cultures of lesioned spinal cord tissue vs normal neuronal tissue from JM #17792 layered over primary rhesus fibroblasts yielded an infectious agent that was identified by transmission EM as a herpesvirus (data not shown). The virus isolate was subsequently passaged and viral DNA purified from cell-free virions for degenerate polymerase chain reaction (PCR) amplification over a highly conserved region of the viral DNA polymerase to identify the virus. Preliminary DNA sequence analysis revealed the virus was most similar to rhesus macaque rhadinovirus (RRV). The complete sequence of the viral genome was determined and compared to simian and human herpesvirus genomes representing alpha-herpesviruses, beta-herpesviruses and gamma-1 and gamma-2 herpesviruses. By this analysis, the JM herpesvirus, referred to as JM rhadinovirus (JMRV) is a gamma-2 herpesvirus most closely related to RRV, with 89.5% nucleotide sequence identity and secondarily related to human Kaposi sarcoma-associated herpesvirus (KSHV) with 47.9% nucleotide sequence identity (Table 2). JMRV has subsequently been isolated from active CNS lesions of 5 other JM with JME, but has not been isolated from normal white matter from JM with or without JME.

Discussion

JME appeared spontaneously in JM at the ONPRC 21 years after the colony was established. The initial case of JME occurred in 1986 and since then the disease typically has affected 1% to 3% of the colony each year, with 2 exceptions. JME usually occurs in young adult animals, but the disease can present in juvenile or aged animals, and shows no preference for either gender. Clinically, JME causes paralysis, ataxia, and ocular motor paresis. While most animals failed to recover sufficiently to be safely returned to the colony, 3 monkeys recovered, were returned to the colony, and then relapsed 1 or more years later. MRI of 8 animals revealed changes similar to acute MS. Pathologically, JME causes multifocal areas of demyelination of varying acuity with loss of oligodendrocytes and variable axonal loss in the white matter of the cerebrum, cerebellum, brainstem, and spinal cord associated with macrophages and lymphocytic infiltrates. Chronic inactive demyelinated lesions also occur, suggesting that asymptomatic lesions may occur before clinical JME. JME is the first naturally occurring inflammatory demyelinating disease in an NHP.

JME has clinical, MRI, and pathologic similarities to MS. These include similar clinical manifestations, a relapsing course in monkeys that recovered sufficiently to be returned to the colony, MRI abnormalities like those of acute MS lesions and similar neuropathologic abnormalities, including plaque-like demyelinating lesions

TABLE 2: Clustal W Alignment of JMRV Genome with Select Simian and Human Herpesvirus Genomes Showing Percent Nucleotide Sequence Identity

Virus	JMRV	RRV	KSHV	HVS	RhLCV	EBV	RhCMV	HHV-6A	HHV-6B	HB virus	SVV	HSV-1
JMRV	100	89.5	47.9	35.0	27.9	22.3	19.5	27.2	26.2	27.1	31.3	25.6
RRV	89.5	100	48.3	34.7	28.3	22.6	19.9	27.6	26.5	27.6	31.5	26.1
KSHV	47.9	48.3	100	32.3	27.3	22.2	19.5	26.7	25.7	27.3	29.3	26.1
HVS	35.0	34.7	32.3	100	20.2	19.4	15.9	23.5	22.8	18.6	30.7	19.4
RhLCV	27.9	28.3	27.3	20.2	100	53.1	23.2	26.1	25.1	28.3	21.7	25.8
EBV	22.3	22.6	22.2	19.4	53.1	100	23.1	22.0	21.3	23.2	20.5	22.7
RhCMV	19.5	19.9	19.5	15.9	23.2	23.1	100	22.3	22.6	20.0	17.0	18.9
HHV-6A	27.2	27.6	26.7	23.5	26.1	22.0	22.3	100	88.3	25.2	24.6	24.0
HHV-6B	26.2	26.5	25.7	22.8	25.1	21.3	22.6	88.3	100	25.0	23.7	23.7
HB virus	27.1	27.6	27.3	18.6	28.3	23.2	20.0	25.2	25.0	100	21.4	49.5
SVV	31.3	31.5	29.3	30.7	21.7	20.5	17.0	24.6	23.7	21.4	100	21.9
HSV-1	25.6	26.1	26.1	19.4	25.8	22.7	18.9	24.0	23.7	49.5	21.9	100

EBV = Epstein Barr virus (GenBank accession number V01555); HB virus = herpes B virus (GenBank accession number NC_004812); HHV-6A = human herpesvirus 6A (GenBank accession number NC_001664); HHV-6B = human herpesvirus 6B (GenBank accession number AF157706); HSV-1 = herpes simplex virus type 1 strain F (GenBank accession number GU734771); HVS = Herpesvirus saimiri (GenBank accession number NC_001350); JMRV = Japanese macaque rhadinovirus (GenBank accession number AY528864.1); KSHV = Kaposi sarcoma-associated herpesvirus (GenBank accession number U75698); RhCMV = rhesus cytomegalovirus (GenBank accession number NC_006150); RhLCV = rhesus lymphocryptovirus (GenBank accession number AY037858); RRV = rhesus macaque rhadinovirus (GenBank accession number AF083501); SVV = simian varicella virus (GenBank accession number NC_002686).

associated with lymphocytes and macrophages, oligodendrocyte depletion, limited remyelination, and variable axonal loss. However, there are some features of JME that differ from MS. These include CSF containing neutrophils as well as lymphocytes in most cases and necrosis and hemorrhage as part of the pathologic continuum. These differences may represent species-specific differences in inflammatory and tissue responses. It is worth noting that EAE in NHP often has neutrophils in the CSF and necrosis and hemorrhage as part of the neuropathology, which differs from EAE in rodents.[18] Overall the clinical, MRI and neuropathologic features of JME have more similarities than differences with MS and JME is clearly an inflammatory demyelinating disease. Further investigations are needed to determine the full extent of similarities of JME with MS.

There are several features of JME that makes this an extremely appealing model for MS. First, the disease occurs spontaneously, which makes it distinct from current models of MS that require artificial manipulation to induce disease. Second, it affects a small percentage of animals in the colony, approximately 1% to 3% each year, suggesting there may be a genetic susceptibility to the disease as there is in MS. The ONPRC began tracing the pedigrees of the JM troop in 2000 utilizing specific microsatellite markers. Interestingly, animals developing JME since 2000 come from distinct matrilines from the original troop, supporting the idea that host genetic factors play a significant part in susceptibility to disease (unpublished data). Determining the genetic factors that coincide with disease and predispose animals to develop JME is currently being explored on archived tissue and new cases. Third, like MS, JME is an inflammatory disease, suggesting either an autoimmune disease or a viral infection. An autoimmune pathogenesis of MS is commonly proposed but definitive evidence of this remains lacking. Autoreactive T cells and anti-myelin antibodies have been proposed as being critical to the immunopathogenesis of MS.[19–21] We are currently assessing new cases of JME for anti-myelin T cell responses and antibodies against myelin antigens.

Finally, based on epidemiologically studies and the histopathology, a viral etiology for MS has long been suspected. Multiple candidate viruses have been proposed but none has been convincingly associated with the disease. Here, we report the isolation of a previously unknown herpesvirus, JMRV, isolated from acute JME

lesions. We have been unable to isolate JMRV from normal appearing white matter of JM with and without JME. Complete DNA sequencing reveals this to be a rhadinovirus with significant sequence homologies with RRV and human KSHV. Reagents are being generated against this virus to evaluate the potential role of JMRV in JME. This is of particular interest since human Epstein-Barr virus and human herpesvirus 6 are 2 herpesviruses that have been implicated as playing a role in the pathogenesis of MS.[22–30] Demonstrating that a simian rhadinovirus induces JME will provide a new class of herpesvirus that would warrant investigation in MS.

In summary, JME is a unique spontaneous demyelinating disease in an NHP. Preliminary results suggest that the disease occurs in genetically predisposed monkeys and is associated with a novel simian herpesvirus. Further investigation of the pathogenesis of JME may provide new insights into the pathogenesis of MS.

Acknowledgments

This research was supported by the National Institutes of Health (NIH/NCRR) Grant P51RR00163 (MKA, SGK, LSS, SWW), the Research Enrichment Award Program of the Department of Veterans Affairs Biomedical Laboratory Research and Development (DNB), the OHSU Multiple Sclerosis Center, the United States Department of Defense (W81XWH-09-1-0276) (LSS, SGK, WDR, SWW), OHSU/Vertex SRA-05-07-01 (WDR) and NIH/NIBIB Grant R01-EB007258 (WDR).

We thank L. Boshears and A. Townsend for assistance with the manuscript and figures, and members of the Division of Animal Resources for their diligence and care of the animals.

Potential Conflicts of Interest

W.D.R. received grants from Vertex Pharmaceuticals and has stock/stock options from DeltaPoint, Inc.

References

1. Noseworthy JH, Lucchinetti C, Rodriguez M, Weinshenker BG. Multiple sclerosis. N Engl J Med. 2000;343:938–952.
2. Libbey J, Fujinami R. Potential triggers of MS. In: Martin R, Lutterotti A, eds. Molecular Basis of Multiple Sclerosis. Berlin/Heidelberg: Springer, 2010:21–42.
3. Libbey JE, Fujinami RS. Experimental autoimmune encephalomyelitis as a testing paradigm for adjuvants and vaccines. Vaccine 2011;29:3356–3362.
4. Ferraro A, Cazzullo CL. Chronic experimental allergic encephalomyelitis in monkeys. J Neuropathol Exp Neurol 1948;7: 235–260.
5. Genain CP, Hauser SL. Creation of a model for multiple sclerosis in Callithrix jacchus marmosets. J Mol Med 1997;75:187–197.
6. Rivers TM, Schwentker FF. Encephalomyelitis accompanied by myelin destruction experimentally produced in monkeys. J Exp Med 1935;61:689–702.
7. 't Hart BA, Massacesi L. Clinical, pathological, and immunologic aspects of the multiple sclerosis model in common marmosets (Callithrix jacchus). J Neuropathol Exp Neurol 2009;68: 341–355.
8. Miller SD, Vanderlugt CL, Begolka WS, et al. Persistent infection with Theiler's virus leads to CNS autoimmunity via epitope spreading. Nat Med 1997;3:1133–1136.
9. Tsunoda I, Fujinami RS. Two models for multiple sclerosis: experimental allergic encephalomyelitis and Theiler's murine encephalomyelitis virus. J Neuropathol Exp Neurol 1996;55: 673–686.
10. Dal Canto MC, Lipton HL. Multiple sclerosis. Animal model: Theiler's virus infection in mice. Am J Pathol 1977;88:497–500.
11. Clatch RJ, Melvold RW, Dal Canto MC, Miller SD, Lipton HL. The Theiler's murine encephalomyelitis virus (TMEV) model for multiple sclerosis shows a strong influence of the murine equivalents of HLA-A, B, and C. J Neuroimmunol 1987;15:121–135.
12. Wong SW, Bergquam EP, Swanson RM, et al. Induction of B cell hyperplasia in simian immunodeficiency virus-infected rhesus macaques with the simian homologue of Kaposi's sarcoma-associated herpesvirus. J Exp Med 1999;190:827–840.
13. Kornek B, Storch MK, Weissert R, et al. Multiple sclerosis and chronic autoimmune encephalomyelitis: a comparative quantitative study of axonal injury in active, inactive, and remyelinated lesions. Am J Pathol 2000;157:267–276.
14. Prineas JW. The neuropathology of multiple sclerosis. In: Koetsier JC (ed). Handbook of Clinical Neurology. Amsterdam: Elsevier, 1985:213–222.
15. Raine CS. Demyelinating diseases. In: (2nd ed.) Davis RL, Robertson DM (Editors). Textbook of Neuropathology. Baltimore, MD: Williams and Wilkins, 1990:468–547.
16. Lucchinetti CF, Bruck W, Rodriguez M, Lassmann H. Distinct patterns of multiple sclerosis pathology indicates heterogeneity on pathogenesis. Brain Pathol 1996;6:259–274.
17. Ozawa K, Suchanek G, Breitschopf H, et al. Patterns of oligodendroglia pathology in multiple sclerosis. Brain 1994;117(Pt 6): 1311–1322.
18. Shaw CM, Alvord EC Jr. Treatment of experimental allergic encephalomyelitis in monkeys. II. Histopathological studies. In: Shiraki H, Yonezawa T, Kuroiwa Y, eds. The Aetiology and Pathogenesis of the Demyelinating Diseases. Tokyo: Japan Science Press, 1976:277–295.
19. Genain CP, Cannella B, Hauser SL, Raine CS. Identification of autoantibodies associated with myelin damage in multiple sclerosis. Nat Med 1999;5:170–175.
20. Diaz-Villoslada P, Shih A, Shao L, Genain CP, Hauser SL. Autoreactivity to myelin antigens: myelin/oligodendrocyte glycoprotein is a prevalent autoantigen. J Neuroimmunol 1999;99: 36–43.
21. Koehler NK, Genain CP, Giesser B, Hauser SL. The human T cell response to myelin oligodendrocyte glycoprotein: a multiple sclerosis family-based study. J Immunol 2002;168:5920–5927.
22. Alvarez-Lafuente R, Martin-Estefania C, de Las Heras V, et al. Active human herpesvirus 6 infection in patients with multiple sclerosis. Arch Neurol 2002;59:929–933.
23. Ascherio A. Epstein-Barr virus in the development of multiple sclerosis. Expert Rev Neurother. 2008;8:331–333.
24. Ascherio A, Munch M. Epstein-Barr virus and multiple sclerosis. Epidemiology 2000;11:220–224.

25. Ascherio A, Munger KL, Lennette ET, et al. Epstein-Barr virus antibodies and risk of multiple sclerosis: a prospective study. JAMA 2001;286:3083–3088.

26. Carrigan DR, Harrington D, Knox KK. Subacute leukoencephalitis caused by CNS infection with human herpesvirus-6 manifesting as acute multiple sclerosis. Neurology 1996;47:145–148.

27. Carrigan DR, Knox KK. Human herpesvirus six and multiple sclerosis. Mult Scler 1997;3:390–394.

28. Cepok S, Zhou D, Srivastava R, et al. Identification of Epstein-Barr virus proteins as putative targets of the immune response in multiple sclerosis. J Clin Invest 2005;115:1352–1360.

29. Challoner PB, Smith KT, Parker JD, et al. Plaque-associated expression of human herpesvirus 6 in multiple sclerosis. Proc Natl Acad Sci U S A 1995;92:7440–7444.

30. Christensen T. The role of EBV in MS pathogenesis. Int MS J 2006;13:52–57.